Elastic anisotropy effects on the electrical responses of a thin sample of nematic liquid crystal

O. A. Gomes,[1] C. A. R. Yednak,[2] R. R. Ribeiro de Almeida,[3] R. T. Teixeira-Souza,[3,*] and L. R. Evangelista[4]

[1]*Departamento de Engenharia Elétrica, Universidade Tecnológica Federal do Paraná, Via do Conhecimento Km 1, 85503-390, Câmpus Pato Branco, Paraná, Brazil*

[2]*Departamento de Física, Universidade Tecnológica Federal do Paraná, Via do Conhecimento Km 1, 85503-390, Câmpus Pato Branco, Paraná, Brazil*

[3]*Departamento de Física, Universidade Tecnológica Federal do Paraná, R. Marcílio Dias, 635, 86812-460, Câmpus Apucarana, Paraná, Brazil*

[4]*Departamento de Física, Universidade Estadual de Maringá, Avenida Colombo, 5790-87020-900, Maringá (PR), Brazil*

(Received 13 September 2016; published 21 March 2017)

The electrical responses of a nematic liquid crystal cell are investigated by means of the elastic continuum theory. The nematic medium is considered as a parallel circuit of a resistance and a capacitance and the electric current profile across the sample is determined as a function of the elastic constants. In the reorientation process of the nematic director, the resistance and capacitance of the sample are determined by taking into account the elastic anisotropy. A nonmonotonic profile for the current is observed in which a minimum value of the current may be used to estimate the elastic constants values. This scenario suggests a theoretical method to determine the values of the bulk elastic constants in a single planar aligned cell just by changing the direction of applied electrical field and measuring the resulting electrical current.

DOI: 10.1103/PhysRevE.95.032704

I. INTRODUCTION

The control of the process of director reorientation with external agents is one of the most important properties of liquid crystals in electronic devices as displays [1,2] and waveguides [3,4]. However, in electrical characterizations, for instance, it can also introduce some difficulties on the experimental data interpretation. In a homogeneous flat sample, below the Fréedericksz threshold, the system behaves as a linear medium. As the critical field is reached, the director reorientation affects both the electric permittivity and the conductivity tensors. Some techniques are employed to avoid this kind of phenomena as, for example, by using an electric field lower than the Fréedericksz threshold [5,6] or by inducing an anchoring orientation parallel to the electric field [7]. Some years ago, the effects of reorientation in electrical responses of nematic sample, in a situation of strong [8] and weak [9] anchoring, have been analyzed. This approach using electrical current responses has been shown to be potentially useful to obtain information about the anchoring energy [9].

In the framework of the elastic continuum theory for nematic liquid crystals, three bulk elastic constants, K_{11}, K_{22}, and K_{33}, are associated to the deformations of splay, twist, and bend, respectively [10,11]. In many theoretical approaches, a very useful approximation is to consider all constants to be alike, thus neglecting effects of the elastic anisotropy. However, this anisotropy is connected to many phenomena observed in liquid crystals, such as spontaneous deformations in cylindrical samples [12,13], blue phases [14], and pattern formation in cholesterics [15], among others. The classical method to measure these elastic constants is based on the Fréedericksz threshold, in which different surface treatments are necessary [16]. Recently, a method was proposed to measure K_{11} and K_{33} by using capacitance measurements and a fitting procedure [17].

In this paper, we study an equivalent electric circuit in a planar cell and propose a simple approach to obtain information about both elastic constants, K_{11} and K_{33}. We assume that the liquid-crystalline cell can be modeled as a resistance, R, associated in parallel to a capacitance, C. Thus the values of these quantities will vary as the deformation is induced in the sample by an external voltage [9]. For this reason, here we deal with the role of elastic anisotropy on the electrical responses of a nematic sample or, more precisely, on the behavior of the resistance, capacitance, and electric current in the presence of an external field. This analysis is performed under the condition of a nonhomogeneous electric field across the sample, which is due to the coupling between the applied electric field and the nematic director [11]. There are several effects influencing the electrical response of the cell, such as adsorption and desorption of ions, i.e., their contribution to the formation of an ionic layer near to the surface sample (Debye layer) and surface inhomogeneity effects, among others [18,19]. For simplicity and in order to focus our attention on the role of the elastic anisotropy, we limit ourselves to the analysis of the reorientation effects. The paper is organized as follows. The dependence of the director profile on the electric voltage is analyzed in Sec. II, whereas in Sec. III the equations for the electric circuit are established. In Sec. IV, the main results of our work are presented and discussed. Section V is dedicated to some concluding remarks.

II. STATEMENT OF THE PROBLEM

For the nematic sample, we consider a slab of thickness d and area A, with the z axis normal to the bounding plates located in $z = \pm d/2$, in a Cartesian reference frame. In this case, in which only *splay-bend* deformations with a planar orientation at the surfaces are considered, ψ is the tilt angle formed by the director with the x axis (parallel to the surfaces), and it is assumed as independent of the y axis. In this scenario, the nematic director may be written as $\mathbf{n} = \cos\psi\,\mathbf{e_x} + \sin\psi\,\mathbf{e_z}$.

*rodolfosouza@utfpr.edu.br

The dynamic reorientation of the director occurs in the presence of a time dependent electrical potential difference $V(t)$ applied to the sample. Consequently, the electric field $\mathbf{E}(z,t) = E(z,t)\mathbf{e_z}$ is responsible for a time dependent molecular reorientation such that $\psi \equiv \psi(z,t)$. Thereby, the bulk free energy due to elastic distortions, accounting for the presence of a time dependent external field, is given by

$$W[\psi,\partial\psi/\partial z;z,t] = \frac{1}{2}\Bigg\{[K_{11}\cos^2\psi(z,t) + K_{33}\sin^2\psi(z,t)]\left(\frac{\partial\psi}{\partial z}\right)^2 - \epsilon_0[\epsilon_\perp + \epsilon_a\sin^2\psi(z,t)]E^2(z,t)\Bigg\}, \quad (1)$$

where K_{11} and K_{33} are the elastic constants associated to the deformations of splay and bend, respectively, ϵ_0 is the dielectric permittivity in the free space, and $\epsilon_a = \epsilon_\parallel - \epsilon_\perp$ is the main dielectric anisotropy, in which $\perp$ and $\parallel$ refer to the direction of the **n**.

A simplified scenario would consider the electric field as uniform across the sample. It is a good approximation for values of the field close to (or much higher than) the Fréedericksz threshold. Here, the discussion is valid for values of the electric field ranging from lower to much higher than the critical one, so the coupling between the electrical field and the nematic director must be taken into account for a more realistic description. The procedure for obtaining the director profile is the one described in [11] and is reproduced here for clarity.

If the time dependence of the electrical potential is slow enough, the viscous torque can be neglected, the quasistatic regime can be adopted [8,9] and the process of minimizing the free energy (1) is the standard variational one. By defining $D = \epsilon_0(\epsilon_\perp + \epsilon_a\sin^2\psi)E(z)$ as the z component of the electric displacement within the sample, it is possible to obtain, through the Euler-Lagrange, the following equation of motion:

$$[K_{11}\cos^2\psi + K_{33}\sin^2\psi]\left(\frac{\partial^2\psi}{\partial z^2}\right) + \sin\psi\cos\psi(K_{33}-K_{11})\left(\frac{\partial\psi}{\partial z}\right)^2 = -\frac{D^2\epsilon_a\sin\psi\cos\psi}{\epsilon_0(\epsilon_\perp+\epsilon_a\sin^2\psi)^2}. \quad (2)$$

For the condition of planar alignment on the surfaces, the maximum distortion occurs in the middle of the sample and we define $\psi(z=0,t) = \psi_m(t)$ because $(d\psi/dz)|_{z=0} = 0$. Integration of Eq. (2) yields

$$\frac{d\psi}{dz} = \frac{\pm D\sqrt{\gamma}}{\sqrt{\epsilon_0\epsilon_\perp K_{11}}} \times \sqrt{\frac{\sin^2\psi_m - \sin^2\psi}{(1+\kappa\sin^2\psi)(1+\gamma\sin^2\psi)(1+\gamma\sin^2\psi_m)}}, \quad (3)$$

in which $\gamma = \epsilon_a\epsilon_\perp^{-1}$ and $\kappa = (K_{33}-K_{11})K_{11}^{-1}$. The positive and negative signs refer to the regions $-d/2 \leqslant z \leqslant 0$ and $0 \leqslant z \leqslant +d/2$, respectively. Furthermore, the electric potential difference can be written as

$$V(t) = 2\int_{-d/2}^{0} E(z,t)dz = \frac{2}{\epsilon_0\epsilon_\perp}\int_{-d/2}^{0}\frac{D(t)}{[1+\gamma\sin^2\psi(z,t)]}dz. \quad (4)$$

By performing the change of variable wherein $\sin^2\chi = (\sin^2\psi/\sin^2\psi_m)$ and inserting Eq. (3) into Eq. (4), it is possible to obtain

$$V = 2\sqrt{\frac{K_{11}}{\epsilon_0\epsilon_a}}(1+\gamma\sin^2\psi_m)^{1/2} \times \int_0^{\pi/2}\sqrt{\frac{1+\kappa\sin^2\chi\sin^2\psi_m}{(1+\gamma\sin^2\chi\sin^2\psi_m)(1-\sin^2\chi\sin^2\psi_m)}}d\chi. \quad (5)$$

The integral in Eq. (5) to be performed numerically establishes the profile of the tilt angle in the middle of the sample, $\psi_m(t)$, as a function of the applied potential $V(t)$. The critical value for the Fréedericksz transition is determined by solving Eq. (5) in the limit of $\psi_m \to 0$, where it is possible to obtain

$$V_c = \pi\sqrt{\frac{K_{11}}{\epsilon_0\epsilon_a}}.$$

This is one of the mechanisms that experimental methods require to measure the elastic constant K_{11}, for a liquid crystal with positive dielectric anisotropy. In fact, for a sample prepared to have planar alignment it is possible to measure also K_{22} by applying an electrical field parallel to the surfaces and perpendicular to the direction of anchoring. For the measurements of K_{33} using the Fréedericksz approach, it is necessary to handle another sample prepared to have homeotropic alignment [16] and the electric field applied parallel to the plates.

III. ELECTRIC PROPERTIES AND ELECTRIC CIRCUIT

If we assume that our nematic cell may be represented by an equivalent circuit, the electric resistance and the capacitance are defined, respectively, by the following equations:

$$R(t) = \frac{1}{A}\int_{-d/2}^{d/2}\frac{dz}{\sigma_{zz}(t)}, \quad C^{-1}(t) = \frac{1}{A}\int_{-d/2}^{d/2}\frac{dz}{\epsilon_0\epsilon_{zz}(t)}. \quad (6)$$

In Eq. (6), $\sigma_{zz}(t) = \sigma_\perp + \sigma_a\sin^2\psi(z,t)$ is the zz component of the conductivity tensor while $\epsilon_{zz}(t) = \epsilon_\perp + \epsilon_a\sin^2\psi(z,t)$ is the zz component of the dielectric tensor in the dielectric medium. Moreover, $\sigma_a = \sigma_\parallel - \sigma_\perp$ is the anisotropy of the conductivity tensor. Inserting Eq. (3) into Eq. (6) and promoting the same change of variable that was performed in the previous section [i.e., $\sin^2\chi = (\sin^2\psi/\sin^2\psi_m)$], it is possible to find the following expressions for $R(t)$ and $C(t)$, respectively:

$$R = \frac{d}{A\sigma_\perp}\left[\frac{K_R(\psi_m)}{J(\psi_m)}\right], \quad C = \frac{A\epsilon_0\epsilon_\perp}{d}\left[\frac{J(\psi_m)}{K_C(\psi_m)}\right], \quad (7)$$

with

$$J(\psi_m) = \int_0^{\pi/2} \sqrt{\frac{(1+\kappa\ \sin^2\chi\ \sin^2\psi_m)(1+\gamma\ \sin^2\chi\ \sin^2\psi_m)}{1-\sin^2\chi\ \sin^2\psi_m}}\, d\chi, \tag{8}$$

$$K_R(\psi_m) = \int_0^{\pi/2} \sqrt{\frac{(1+\kappa\ \sin^2\chi\ \sin^2\psi_m)(1+\gamma\ \sin^2\chi\ \sin^2\psi_m)}{(1+\varrho\ \sin^2\chi\ \sin^2\psi_m)^2(1-\sin^2\chi\ \sin^2\psi_m)}}\, d\chi, \tag{9}$$

$$K_C(\psi_m) = \int_0^{\pi/2} \sqrt{\frac{(1+\kappa\ \sin^2\chi\ \sin^2\psi_m)}{(1+\gamma\ \sin^2\chi\ \sin^2\psi_m)(1-\sin^2\chi\ \sin^2\psi_m)}}\, d\chi, \tag{10}$$

in which $\varrho = \sigma_a/\sigma_\perp$.

As mentioned earlier, in this approximation, the nematic sample behaves as a parallel circuit, where the resistance $R(t)$ and the capacitance $C(t)$ are subject to the same voltage. This yields a total current $I(t)$ across the sample in the form

$$I(t) = \left[\frac{1}{R(t)} + \frac{dC(t)}{dt}\right]V(t) + C(t)\frac{dV(t)}{dt}, \tag{11}$$

where the first and the second terms are the resistive and capacitive current, respectively.

A complete description of the electrical responses of an ordinary nematic sample, even in the quasistatic regime, should consider ionic adsorption effects inside the sample. Due to the accumulation of ions near the surfaces, a thin double layer with the thickness of the Debye's length appears at each surface, and this would reduce the voltage inside the nematic sample [18–20]. The length of the double layer depends, among other parameters, on the ion concentration.

As pointed out before, we are addressing our attention only to reorientation effects caused by the electric field in order to analyze the effects of the elastic anisotropy. Thus our approximation is valid for a sample filled with a very weakly ionized material (like most liquid crystals [21]).

IV. ELECTRICAL RESPONSE CHARACTERIZATION

In order to analyze the electrical properties of this sample, let us consider the effect of a linearly increasing potential $V(t) = (V_0/T)t$, where V_0 is the potential for $t = T$. For simplicity, we use $V_0 = 10$ V and $T = 10$ s. Moreover, we consider also some typical values for the parameters characterizing the cell, as indicated in Table I [8]. The numerical procedures were performed with the software Mathematica® with standard precision and no problem of convergence was encountered.

The profile of $\psi_m(t)$, obtained from Eq. (5), is shown in Fig. 1, for different values of κ. As expected, it is possible to identify the Fréedericksz transition in the behavior of ψ_m as a function of t. Indeed, before the transition $t < t_c$, one can observe the uniform orientation, i.e., $\psi_m = 0$. When $t \geqslant t_c$, one observes that $\psi_m > 0$, which leads to a distortion in the middle of the sample.

It is possible to verify that $\psi_m \to \pi/2$ when $t \to \infty$, but when $t \to T$, its asymptotic value is practically reached [11], which means that the tilt angle in the middle of the sample is perpendicular to the orientation of the surface, as denoted in Fig. 1 by a saturation behavior. A distinguished feature of Fig. 1 may be identified by the different response times of the director profile according to the applied electrical field. Since $\kappa = (K_{33} - K_{11})/K_{11}$, when $\kappa < 0$, the privileged elastic deformation is of the *bend* type. This implies that the molecular reorientation along the electric field direction is favored. In fact, when the elastic energy and the electric field favor the molecular reorientation in the same direction, it results in a faster electrical response shown in Fig. 1. On the other hand, when $\kappa > 0$, the larger elastic constant is K_{33} and the molecular reorientation is favored along the direction perpendicular to the applied electric field. It is worth mentioning that, in this case, there is a competition among the elastic energy and the applied electric field, which results in the slower electrical response depicted in Fig. 1.

The behavior of $R(t)$ and $C(t)$ can be obtained by means of Eqs. (7) and their profiles are illustrated in Figs. 2(a) and 2(b), respectively. From Eq. (11) we obtain the electric current through the sample and its profile is shown in Fig. 3.

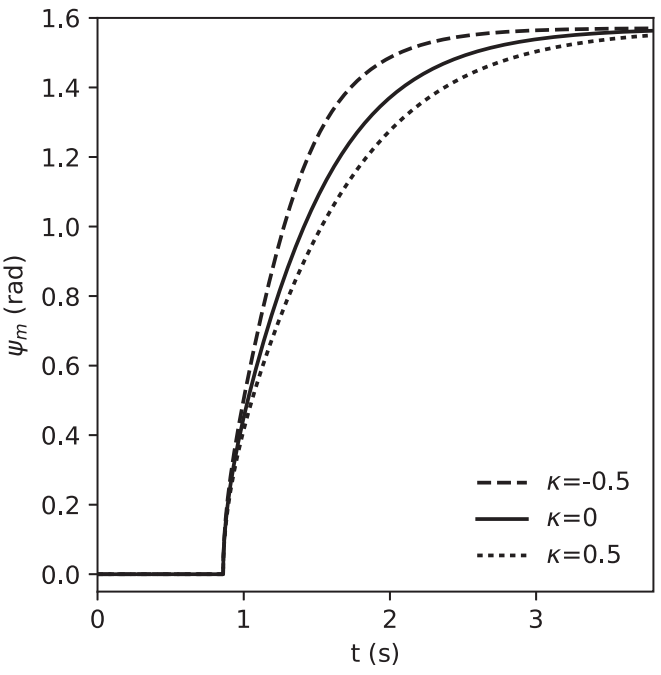

FIG. 1. Behavior of the tilt angle profile $\psi_m(t)$ vs $t(s)$, for different values of κ and the parameters presented in Table I. The discontinuity observed occurs at time $t = t_c \approx 0.8592$ s, which coincides with the time that $V(t)$ reaches V_c for these parameters.

TABLE I. Physical parameters used in numerical experiments.

Parameter	A	d	K_{11}	$\epsilon_{\parallel}$	$\epsilon_{\perp}$	$\sigma_{\parallel}$	$\sigma_{\perp}$
Value	10^{-4} m^2	5×10^{-6} m	10^{-11} N	20.6	5.5	$10^{-10}(\Omega\,\mathrm{m})^{-1}$	$5\sigma_{\parallel}$

It is important to note in Fig. 3 the presence of a sharp transition when $t = t_c$. This discontinuity is due to the term $dC(t)/dt$ present in Eq. (11), as discussed in [8]. Another interesting feature observed here is that the amplitude of the discontinuity varies with κ in a decreasing rate, even the slight one, which is evidenced in the inset of Fig. 3. The origin of this change on the amplitude of the discontinuity can be observed in Fig. 4, where we present the term connected to the derivative of the capacitance in Eq. (11).

A much more prominent effect of the elastic anisotropy on the electric current behavior is the nonmonotonic profile above the Fréedericksz transition. After the arising of the discontinuity, the electric current is still increasing with time until reaching a maximum point, which is then followed by a local minimum. The values of the current and time associated to this minimum depend on the different values of κ. To investigate the origin of this minimum, we notice that there are three terms forming the total electric current expression in Eq. (11). The two first terms, which are multiplied by $V(t)$, are the resistive part, while the last term is the capacitive part. According to our numerical values, the capacitive term coincides with the capacitance profile, and it makes no contribution to the nonmonotonic behavior of the current. Figure 4(b) show that the purely resistive part of the current, $V(t)/R(t)$, is responsible for this local minimum. Physically, one should expect an increase of the electric current with the voltage. In fact, the decreasing of the electric current is given by the negative value of σ_a. After the threshold, as the conductivity decreases, the resistance increases and it influences the electric current. When the voltage increases, the competition between voltage and resistance produces this nonmonotonic behavior in the electric current. The electric-current characteristics should

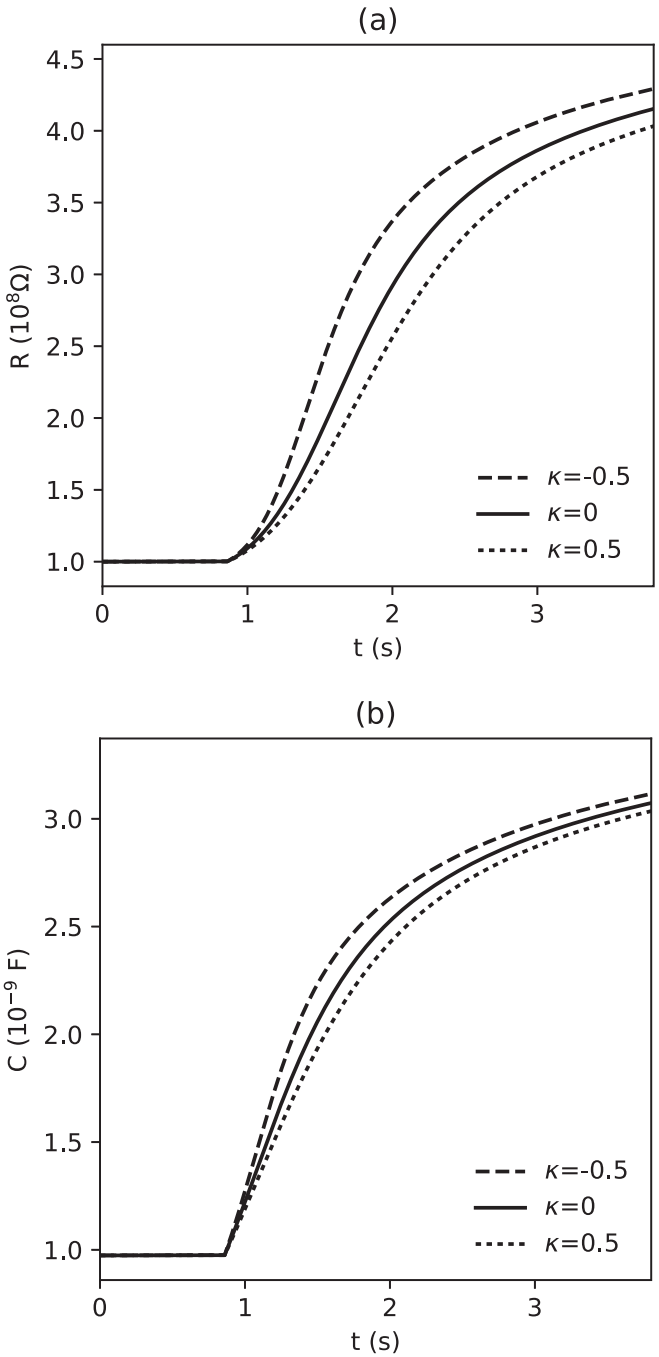

FIG. 2. (a) Behavior of the resistance $R(t)$ vs $t(s)$, for different values of κ, and (b) behavior of the capacitance $C(t)$ vs $t(s)$, for different values of κ. The physical parameters are given in Table I.

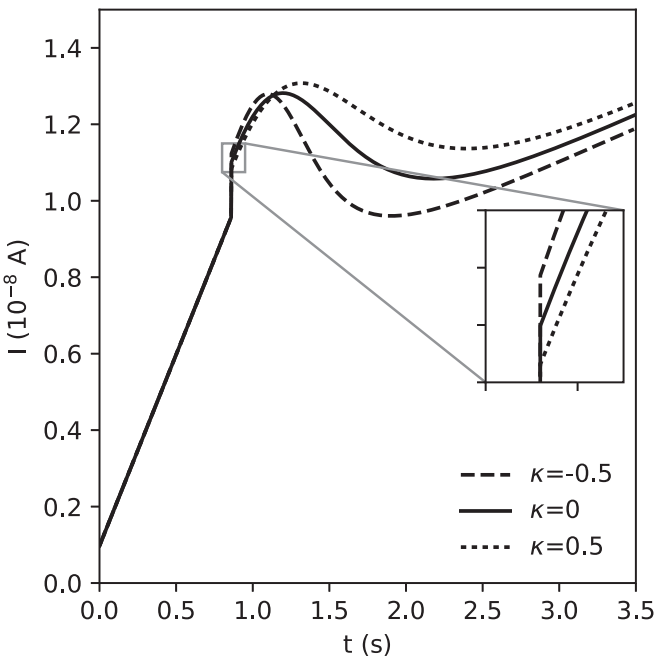

FIG. 3. Behavior of the intensity of the electric current $I(t)$ vs $t(s)$, for different values of κ and physical parameters presented in Table I. The highlighted part shows more clearly the behavior immediately below and above of the Fréedericksz threshold.

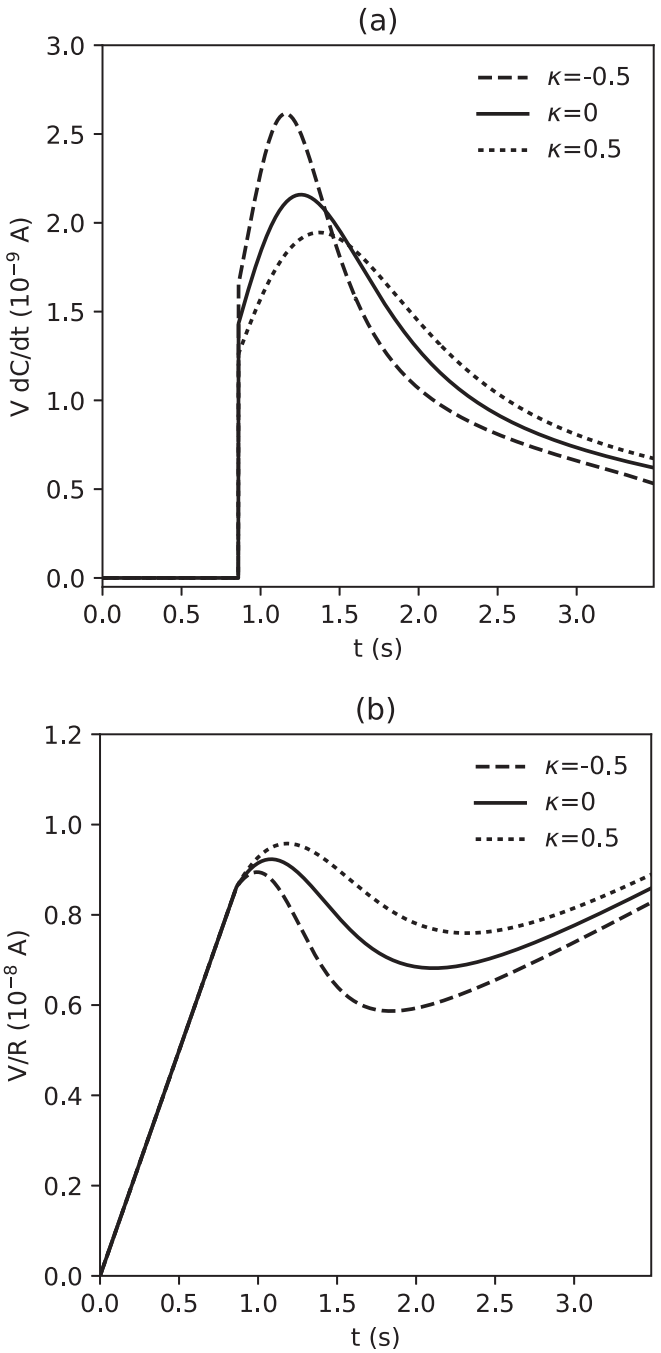

FIG. 4. Separate profiles of the contributions to electric current from Eq. (11) evidencing (a) the amplitude of the discontinuity, and (b) the concavity observed in Fig. 3. The capacitive part of the electric current coincides with the profile of capacitance due the fact that $dV/dt = 1$.

be different if the anisotropy in the conductivity is positive. In that case, both voltage and the decrease in resistance tend to increase the electric current, and no minimum would be found.

Figure 3 shows that the minimum found in the electrical current moves to the right when κ increases, i.e., when the *splay* elastic distortion begins to prevail, the electrical current increases. This makes perfect sense when we take into account Fig. 2. The higher the value of κ, the lower the resistance, which

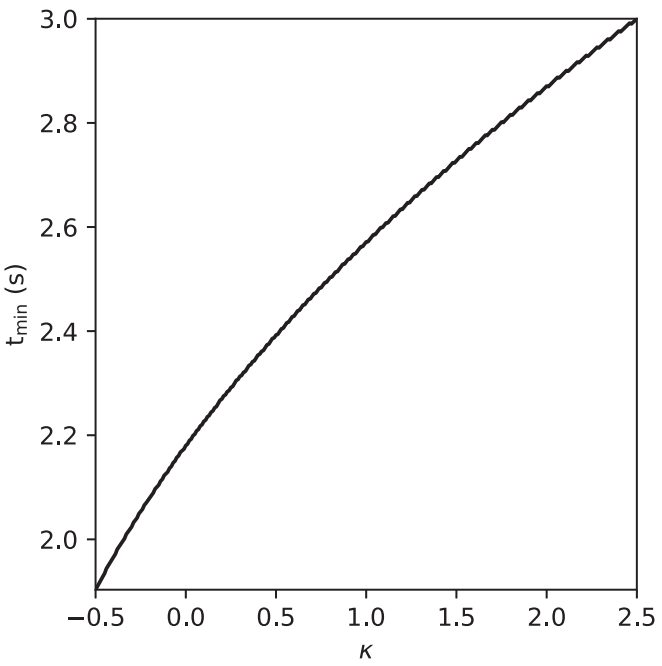

FIG. 5. Behavior of the time in which the minimum occurs vs κ. Physical parameters are given in Table I.

fits perfectly with Ohm's law. Then, we can build a profile for the value of $t_{\min}$ in which the minimum is observed as a function of the elastic parameter κ. This behavior is shown in Fig. 5, for the set of parameters used in our analysis. This figure shows that in the range from $\kappa = -0.5$ ($K_{33}/K_{11} = 0.5$) to $\kappa = 2.5$ ($K_{33}/K_{11} = 3.5$), $t_{\min}$ varies from approximately 1.9 s to 3.0 s. This feature could be useful to estimate the values of the ratio K_{33}/K_{11}. In this way, once the value of K_{11} is obtained from the Fréedericksz transition, our numerical results indicate the possibility of estimating the value of K_{33} as well with a single sample and a single measurement of the electric current. In principle, the value of K_{33} can be extracted from this electric current analysis; however, as the model considers some approximations (as, e.g., the strong anchoring), this value should present a slight deviation from the measured value in the standard method. In fact, this approach can be useful as a preliminary characterization of the elastic proprieties of the sample. Once K_{11} has been measured with the threshold potential, one can obtain some information about the bend elastic constant by increasing the voltage until the minimum of current is reached.

V. CONCLUSIONS

We have investigated the electrical properties, more specifically, the behavior of the resistance, capacitance, and total electric current of a pure sample of nematic liquid crystals in the presence of an external field. The analysis was developed by considering the coupling of the electric field and the nematic director, which results in a nonuniform distribution of the electric field across the sample. We have investigated the role of the elastic anisotropy on these electrical properties. Our studies indicate a significant change in the profiles of electric current according to the values of the ratio between the K_{33}

and K_{11} elastic constants. Indeed, a nonmonotonic behavior of the electric current is observed, in which a minimum value is found for an electric voltage only few times larger than the Fréedericksz threshold. We have shown that this minimum occurs for different values of voltage as the elastic constants ratio varies. The time profile of this minimum is built as a function of the elastic parameters, showing that it changes significantly for different values of elastic constants. This behavior suggests that it is possible to use electric current measurements to yield estimates of both elastic constants, K_{11} and K_{33}, if we assume that the value of one of them is obtained from the critical voltage.

ACKNOWLEDGMENTS

The authors are thankful to Brazilian agencies CNPq (RTT-S Grant No. 443339/2014-7) and CAPES. O.A.G. is grateful to Fundação Araucária and L.R.E. thanks the INCT-FCX (National Institute of Science and Technology in Complex Fluids) Grant No. 573560/2008-0 for financial support.

[1] G. P. Bryan-Brown, C. V. Brown, I. C. Sage, and V. C. Hui, Nature (London) **392**, 365 (1997).
[2] T.-J. Chen, G.-J. Lin, B.-Y. Chen, B.-R. Lin, J.-J. Wu, and Y.-J. Yang, Displays **37**, 94 (2015).
[3] M. Warenghem, J. F. Henninot, and G. Abbate, Opt. Express **12**, 483 (1998).
[4] C.-C. Shih, Optik **127**, 2393 (2016).
[5] R. Atasiei, A. L. Alexe-Ionescu, J. C. Dias, L. R. Evangelista, and G. Barbero, Chem. Phys. Lett. **461**, 164 (2008).
[6] F. Carbone, A. Mazzulla, F. Ciuchi, and N. Scaramuzza, Eur. Phys. J. Plus **130**, 151 (2015).
[7] P. P. Korneychuk, A. M. Gabovich, A. I. Voitenko, and Yu. A. Reznikov, Ukr. J. Phys. **54**, 75 (2008).
[8] R. Atasiei, A. L. Alexe-Ionescu, C. Dascalu, J. C. Dias, and R. T. de Souza, Phys. Lett. A **372**, 6116 (2008).
[9] R. T. de Souza, M. M. A. de Jesus, J. C. Dias, and L. R. Evangelista, Phys. Rev. E **80**, 041702 (2009).
[10] G. Barbero and L. R. Evangelista, *An Elementary Course on The Continuum Theory For Nematic Liquid Crystals*, Series on Liquid Crystals Vol. 3 (World Scientific, Singapore, 2001).
[11] I. W. Stewart, *The Static and Dynamic Continuum Theory of Liquid Crystals: A Mathematical Introduction*, Liquid Crystals Book Series (Taylor & Francis, London, 2004).
[12] D. R. M. Williams and A. Halperin, Phys. Rev. E **48**, R2366 (1993).
[13] C. Chiccoli, P. Pasini, L. R. Evangelista, R. T. Teixeira-Souza, and C. Zannoni, Phys. Rev. E **91**, 022501 (2015).
[14] J. I. Fukuda, Phys. Rev. E **85**, 020701 (2012).
[15] R. S. Zola, L. R. Evangelista, Y.-C. Yang, and D.-K. Yang, Phys. Rev. Lett. **110**, 057801 (2013).
[16] P. G. de Gennes, *The Physics of Liquid Crystals* (Oxford Press, London, 1974).
[17] K. Iwava, H. Naito, H. Ichinose, M. Klasen-Memmer, and K. Tarumi, Proc. 16th Int. Display Workshops **1**, 229 (2009).
[18] G. Barbero, G. Cipparrone, O. G. Martins, P. Pagliusi, and A. M. Figueiredo Neto, Appl. Phys. Lett. **89**, 132901 (2006).
[19] G. Barbero and L. R. Evangelista, *Adsorption Phenomena and Anchoring Energy in Nematic Liquid Crystals* (Taylor & Francis Group, Boca Raton, FL, 2006).
[20] R. R. Ribeiro De Almeida, L. R. Evangelista, and G. Barbero, Phys. Lett. A **376**, 3382 (2012).
[21] A. Jákli and A. Saupe, *One- and Two-Dimensional Fluids: Properties of Smectic, Lamellar and Columnar Liquid Crystals* (CRC Press, Boca Raton, FL, 2006).